Hepatic stearoyl CoA desaturase 1 deficiency increases glucose uptake in adipose tissue partially through the PGC-1α–FGF21 axis in mice

Received for publication, July 8, 2019, and in revised form, October 22, 2019 Published, Papers in Press, November 5, 2019, DOI 10.1074/jbc.RA119.009868

Ahmed Aljohani[‡§1], **Mohammad Imran Khan**[¶‖], **Abram Bonneville**[**], **Changan Guo**[**], **Justin Jeffery**[‡‡], **Lucas O'Neill**[**], **Deeba Nadeem Syed**[¶], **Sarah A. Lewis**[**], **Maggie Burhans**[§§], **Hasan Mukhtar**[¶], and **James M. Ntambi**[**§§2]

From the [‡]*Endocrinology and Reproductive Physiology Graduate Training Program and* [¶]*Department of Dermatology, School of Medicine and Public Health, University of Wisconsin, Madison, Wisconsin 53706, the* [§]*College of Science and Health Professions, King Saud bin Abdulaziz University for Health Sciences, Riyadh 11481, Saudi Arabia, the* [‖]*Department of Biochemistry, Faculty of Science, King Abdulaziz University, Jeddah, Saudi Arabia, the Departments of* [**]*Biochemistry and* [§§]Nutritional Sciences and [‡‡]*Carbone Cancer Center,University of Wisconsin, Madison, Wisconsin 53706*

Edited by Qi-Qun Tang

Increased carbohydrate consumption increases hepatic *de novo* lipogenesis, which has been linked to the development of chronic metabolic diseases, including obesity, hepatic steatosis, and insulin resistance. Stearoyl CoA desaturase 1 (SCD1) is a critical lipogenic enzyme that catalyzes the synthesis of two monounsaturated fatty acids, oleate and palmitoleate, from the saturated fatty acids stearate and palmitate, respectively. SCD1-deficient mouse models are protected against diet-induced adiposity, hepatic steatosis, and hyperglycemia. However, the mechanism of this protection by SCD1 deficiency is unclear. Using liver-specific SCD1 knockout (LKO) mice fed a high-carbohydrate, low-fat diet, we show that hepatic SCD1 deficiency increases systemic glucose uptake. Hepatic SCD1 deficiency enhanced glucose transporter type 1 (GLUT1) expression in the liver and also up-regulated GLUT4 and adiponectin expression in adipose tissue. The enhanced glucose uptake correlated with increased liver expression and elevated plasma levels of fibroblast growth factor 21 (FGF21), a hepatokine known to increase systemic insulin sensitivity and regulate whole-body lipid metabolism. Feeding LKO mice a triolein-supplemented but not tristearin-supplemented high-carbohydrate, low-fat diet reduced FGF21 expression and plasma levels. Consistently, SCD1 inhibition in primary hepatocytes induced FGF21 expression, which was repressed by treatment with oleate but not palmitoleate. Moreover, deletion of the transcriptional coactivator PPARγ coactivator 1α (PGC-1α) reduced hepatic and plasma FGF21 and white adipocyte tissue-specific GLUT4 expression and raised plasma glucose levels in LKO mice. These results suggest that hepatic oleate regulates glucose uptake in adipose tissue either directly or partially by modulating the hepatic PGC-1α–FGF21 axis.

Obesity is a worldwide health problem. There is abundant evidence that obese individuals are more susceptible to developing chronic metabolic diseases, including insulin resistance, type 2 diabetes, cardiovascular disease, and nonalcoholic fatty liver disease (NAFLD)[3] (1). There are several factors that influence weight gain, including dietary, genetic, lifestyle and environmental variables, which, in turn, affect food intake and energy expenditure. Attempts to reduce fat consumption usually accompanies increased carbohydrate intake, which significantly enhances endogenous hepatic *de novo* lipogenesis (DNL). Accordingly, high-carbohydrate diet (HCD)–induced adiposity and hepatic steatosis are partially attributed to increased hepatic DNL, followed by very-low-density lipoprotein–mediated transport of triglyceride to white adipose tissue (WAT). Moreover, DNL is a source of liver fat accumulation, leading to NAFLD associated with hepatic insulin resistance and enhanced glucose intolerance (2, 3). NAFLD patients exhibit increased liver expression of lipogenic genes, including sterol regulatory element–binding protein 1 (SREBP1), stearoyl CoA desaturase 1 (SCD1), and fatty acid synthase (4).

Monounsaturated fatty acids (MUFAs) are the major substrates for complex lipid synthesis, including triglycerides, phospholipids, cholesterol esters, and wax esters. SCD1, the central enzyme in lipogenesis, catalyzes the rate-limiting step in MUFA synthesis. It desaturates saturated fatty acids (SFAs), mainly stearate (18:0) and palmitate (16:0), into MUFAs, oleate (18:1n9) and palmitoleate (16:1n7), respectively. SCD1 expression is highly responsive to different stimuli that trigger or suppress liver lipogenesis. The SCD1 desaturation index, the ratio

This work was supported by National Institutes of Health Grants R01 DK062388 and DK118093, American Diabetes Association Grant 7-13-BS-118, and Department of Agriculture Hatch Grant W2005 (to J. M. N.). The authors declare that they have no conflicts of interest with the contents of this article. The content is solely the responsibility of the authors and does not necessarily represent the official views of the National Institutes of Health.

This article contains Figs. S1 and S2.

[1] Supported by a Saudi Cultural Mission SACM fellowship and United States Public Health Service Grant R01 AR059742 (to H. M).

[2] To whom correspondence should be addressed. E-mail: james.ntambi@wisc.edu.

[3] The abbreviations used are: NAFLD, nonalcoholic fatty liver disease; DNL, *de novo* lipogenesis; HCD, high carbohydrate diet; WAT, white adipose tissue; MUFA, monounsaturated fatty acid; SFA, saturated fatty acid; BAT, brown adipose tissue; LKO, liver-specific knockout; GKO, global knockout; ChREBP, carbohydrate response element–binding protein; CT. computed tomography; FDG, 2-deoxy-2-[^{18}F]fluoro-d-glucose; ER, endoplasmic reticulum; DLKO, double liver knockout; ID, injected dose.

of MUFAs to SFAs, shows a positive correlation with changes in human body adiposity and insulin resistance (5–7). Similarly, a number of studies have reported a positive correlation of the SCD1 desaturation index with human plasma triglycerides or dyslipidemia in patients with familiar combined hyperlipidemia, suggesting that excess MUFAs may contribute to the development of metabolic diseases (8–10). Despite this controversy, accumulating evidence indicating its involvement in the regulation of body weight validates the need to study SCD1 as a potential molecular target in lipid-associated metabolic disorders.

We have shown previously that global deletion of SCD1 protects against diet-induced adiposity and hepatic steatosis despite hyperphagia being observed in SCD1-deficient mice. This protection is associated with decreased hepatic DNL, enhanced fatty acid oxidation, and increased energy expenditure (11). Furthermore, global SCD1 deletion elevates insulin signaling and increased glucose uptake in muscle and brown adipose tissue (BAT) (12). An increased glucose uptake phenotype has also been observed in the heart in response to global SCD1 deletion (13).

To further understand the role of hepatic MUFAs in the regulation of systemic glucose metabolism in response to an HCD, we created a mouse model of SCD1 liver tissue–specific knockout (LKO) mice. Employing this model, we showed that hepatic SCD1 deficiency protects against HCD-induced hepatic steatosis and improves insulin sensitivity (14, 15). Reduced hepatic MUFA levels prevent the normal insulin–SREBP1c–mediated lipogenic response, resulting instead in a dramatic decrease in the rate of fatty acid synthesis. Despite continuous ingestion of the HCD, the block in hepatic DNL was paradoxically associated with hypoglycemia and reduced levels of hepatic glycogen (15, 16). Here we show that hepatic SCD1 deficiency increases glucose uptake in the liver and adipose tissue through GLUT1 and GLUT4, respectively. The increased systemic glucose uptake correlates with elevated hepatic expression and plasma levels of FGF21, which were reduced upon feeding triolein- but not tristearin-supplemented HCD. Furthermore, oleate suppressed the expression of FGF21 caused by SCD1 inhibition in primary hepatocytes, whereas FGF21 expression remained elevated in the cells cotreated with an SCD1 inhibitor and palmitate or palmitoleate. Hepatic PGC-1α deletion reduced FGF21 gene expression and partially increased basal glucose levels in LKO mice. Our data shed light on the regulatory effect(s) of hepatic oleate on glucose uptake and identify liver PGC-1α, FGF21, and adiponectin as its downstream targets.

Results

Hepatic SCD1 deficiency enhances systemic glucose uptake

We have shown previously that global SCD1 deficiency protects against diet-induced adiposity and improves glucose metabolism. SCD1 global knockout (GKO) mice demonstrate increased glucose uptake in BAT, heart, and skeletal muscle (12, 13, 17). Given that SCD1 is deleted from all tissue, using GKO mice alone was not sufficient to determine the individual contribution of SCD1 from different tissues to these phenotypes. To do so, we used LKO mice to investigate the role of hepatic SCD1 in regulating glucose metabolism. LOX control and LKO mice were fed an HCD for 10 days, and then an *in vivo* 2-[^{3}H]deoxyglucose uptake assay was performed at the end of the feeding period. All mice were fasted for 4 h before receiving oral gavage (15 μCi/mouse) of 2-[^{3}H]deoxyglucose in 20% dextrose solution. Mice were euthanized after 1.5 h, and radioactivity was quantified in collected tissues using the liquid scintillation counter. Liver, spleen, WAT, and BAT of LKO mice showed increased glucose uptake relative to the corresponding tissues of LOX control mice (Fig. 1). Brain tissue of LKO mice showed a trend toward increased glucose uptake ($p = 0.068$). No significant change was observed in glucose uptake in the muscle and heart of LKO mice. Our data indicate that hepatic SCD1 deficiency results in increased glucose uptake in the liver and extrahepatic tissues like WAT and BAT.

Hepatic SCD1 differentially regulates genes encoding glucose transporters in metabolic tissues

To determine how hepatic SCD1 deficiency enhances glucose uptake in metabolic tissues, we measured the expression of glucose transporter genes in the liver, WAT and BAT. Livers of LKO mice fed an HCD demonstrated increased GLUT1 expression and decreased GLUT2 expression (Fig. 2*A*). On the other hand, in WAT, hepatic SCD1 deficiency caused significant upregulation of GLUT4 gene and protein expression and showed no effect on GLUT1 expression (Fig. 2, *B* and *C*). The BAT of LKO mice showed a similar trend, displaying increased GLUT4 protein expression ($p = 0.054$) (Fig. 2*D*). Next, to determine whether increased glucose uptake is associated with enhanced lipogenesis, we measured the expression of lipogenic genes in adipose tissues. A gene expression analysis performed using WAT and BAT of LKO mice showed no significant alteration in the levels of carbohydrate response element–binding protein (ChREBP) α and ChREBP β or elongation of very-long-chain fatty acid protein (ELOV) 5 and ELOV 6 compared with control mice (Fig. 2, *E* and *F*). The relative expression of other lipogenic genes, such as SCD1 and fatty acid synthase 1 (FASN) were unchanged (14). Taken together, our study suggests that, during 10- to 14-day feeding of a high-carbohydrate, low-fat diet, hepatic SCD1 deficiency has little effect on the expression of lipogenic genes in WAT and BAT of LKO mice.

Hepatic SCD1 deficiency enhances systemic glucose uptake through GLUT1-dependent and -independent mechanisms

To further investigate the role of GLUT1 in hepatic SCD1 deficiency–induced glucose uptake in liver and adipose tissues, we performed PET/computed tomography (PET/CT) scanning using 2-deoxy-2-[^{18}F]fluoro-D-glucose (FDG). Animals maintained on an HCD for 10 days were fasted overnight prior to intravenous injection of either vehicle or the GLUT1 inhibitor phloretin (10 mg/kg of body weight) (18). After 1 h, mice were injected with ~9 MBq of FDG before performing imaging studies. Consistent with the 2-[^{3}H]deoxyglucose uptake study, livers of LKO mice showed increased glucose uptake compared with livers of control LOX mice. This induction of glucose uptake was reduced to control levels upon phloretin treatment, which suggests that SCD1 deficiency induces glucose uptake in the liver through recruitment of GLUT1 (Fig. 3, S1). Further-

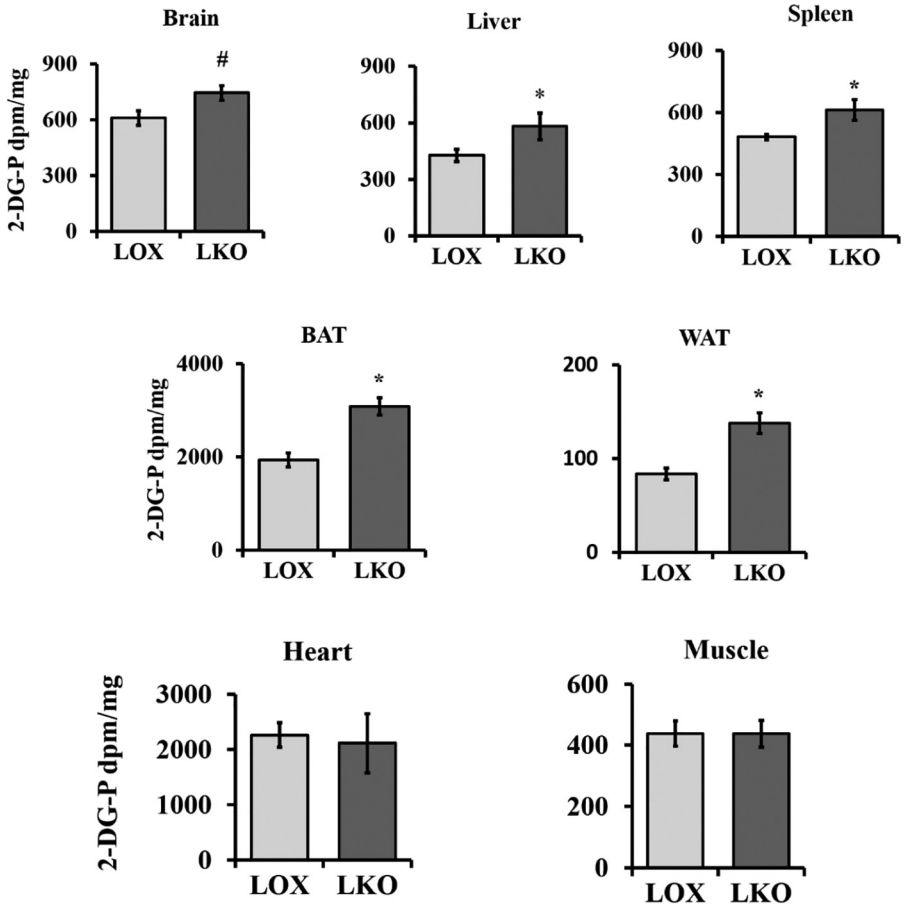

Figure 1. Hepatic SCD1 deficiency enhances systemic glucose utilization. 10-week-old LOX and LKO male mice were fed an HCD for 10 days. Mice fasted 4 h before an oral gavage dose of 15 μCi/mouse of 2-[^{3}H]deoxyglucose in 20% dextrose solution. Tissues were collected after 90 min, and radiolabel activity was measured by liquid scintillation counter. (n = 3/group). Values are mean ± S.E. *, $p < 0.05$; #, $p = 0.068$ *versus* LOX counterparts by Student's two-tailed t test.

more, we observed a similar increase in glucose uptake in the small intestine and WAT of LKO animals, reduced to control levels in the former but not the latter upon phloretin treatment (Fig. 3). This indicates that increased glucose uptake in WAT is independent of GLUT1. Similarly, comparative studies in the brain demonstrated more glucose uptake in LKO compared with LOX mice. However, there was no appreciable difference in glucose uptake levels between phloretin-treated animals, suggesting a redundant role of GLUT1 in the brain of LKO mice (Fig. 3).

Hepatic SCD1 deficiency induces FGF21 and plasma adiponectin expression

Next we assessed the effect of hepatic SCD1 deficiency on the expression of genes encoding hepatokines shown previously to enhance systemic glucose metabolism. LKO mice fed an HCD showed higher expression of hepatic FGF21 compared with LOX control mice (Fig. 4*A*). The increase in hepatic FGF21 expression correlated with a similar elevation of plasma FGF21 levels in LKO mice (Fig. 4*A*). Consistent with elevated plasma FGF21 and, possibly, increased FGF21 signaling, LKO mice showed higher hepatic expression of fibroblast growth factor coreceptor β Klotho (KLB) (Fig. 4*B*). To determine the source of elevated FGF21 plasma levels and probable contribution of other tissues, we measured the expression of FGF21 in adipose tissues. Interestingly, there was no change in FGF21 expression in WAT and BAT of LKO mice compared with tissues from LOX mice (Fig. 4*C*). This suggested that increased circulating plasma FGF21 levels in LKO mice are mainly derived from the liver. Next we investigated the effect of elevated plasma FGF21 on WAT metabolism. We measured the expression of adiponectin in WAT, which has been shown to be increased upon FGF21 treatment (19). Adiponectin expression was significantly increased in adipose tissue of LKO relative to WAT of LOX mice. Accordingly, plasma adiponectin levels were increased in LKO compared with LOX animals (Fig. 4*D*).

Oleate is a critical regulator of FGF21 expression

We have reported previously that hepatic SCD1 deficiency protects against HCD-induced obesity and hepatic steatosis (15). The body weights of LKO mice fed a high CHO diet for 10 days were reduced (Fig. S2). The reduced body weight of LKO mice correlates with decreased DNL and reduced hepatic lipogenic gene expression (15). The precise mechanism(s) by which hepatic SCD1 deficiency reduces the expression of lipogenic genes and subsequently suppresses hepatic lipogenesis is not known. We showed previously that, when LKO mice were fed a triolein-supplemented HCD, expression of lipogenic genes and adiposity was restored to control levels (15). Because an exogenous source of oleate restored lipogenesis in LKO mice, we

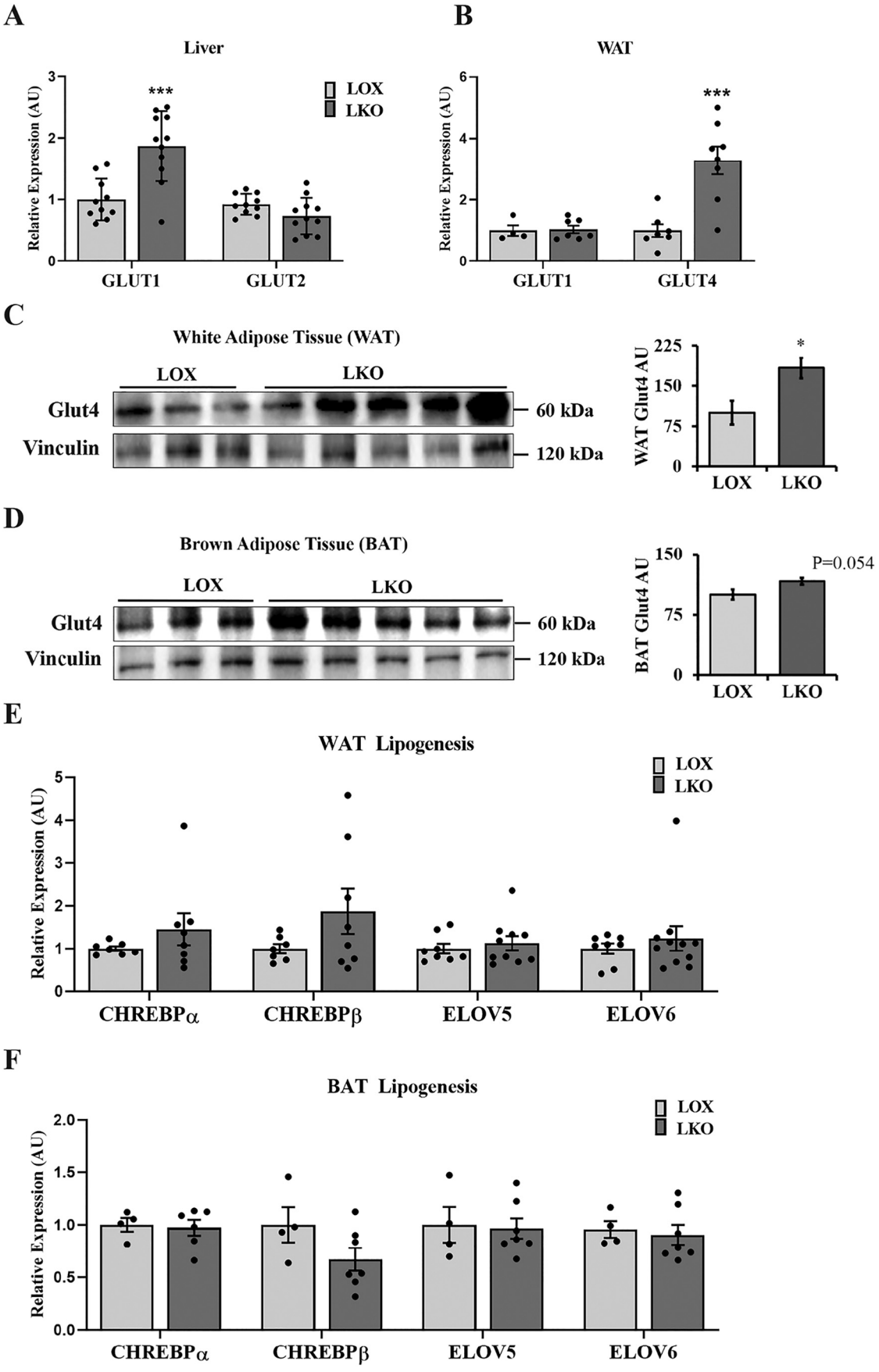
A
Liver
Relative Expression (AU)
LOX
LKO
***
GLUT1
GLUT2
B
WAT
Relative Expression (AU)
***
GLUT1
GLUT4
C
White Adipose Tissue (WAT)
LOX
LKO
Glut4
Vinculin
60 kDa
120 kDa
WAT Glut4 AU
*
D
Brown Adipose Tissue (BAT)
BAT Glut4 AU
P=0.054
E
WAT Lipogenesis
CHREBPα
CHREBPβ
ELOV5
ELOV6
F
BAT Lipogenesis

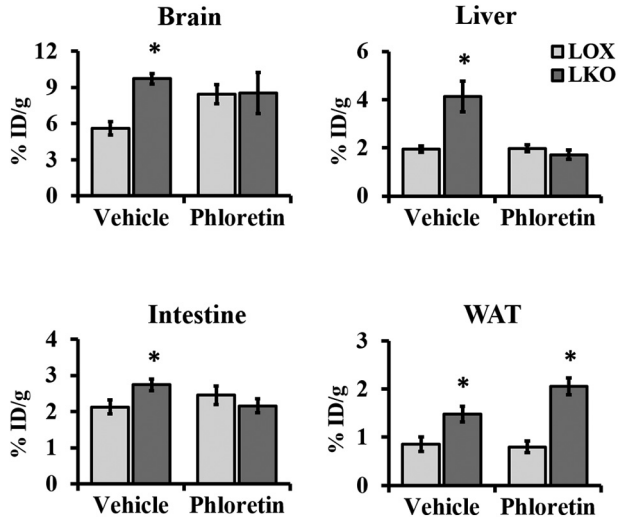

Figure 3. Hepatic SCD1 deficiency enhances glucose uptake through GLUT1-dependent and -independent mechanisms. 12-week-old LOX and LKO mice were fed an HCD for 10 days and fasted overnight prior to an intravenous injection of either vehicle or phloretin (10 mg/kg of body weight). One hour after phloretin treatment, mice received an intravenous injection of FDG 1 h before imaging. FDG uptake levels were quantified as the percent injected dose normalized by the mass of the tissue of interest. Values are mean ± S.E. (n = 4–6/group). *, $p < 0.05$ *versus* LOX counterparts by Student's two-tailed t test.

asked whether hepatic SCD1 deficiency decreases DNL through up-regulation of FGF21 expression. We hypothesized that triolein feeding decreases FGF21 expression in the liver of LKO mice. To test this hypothesis, we fed LOX and LKO mice either an HCD, a triolein-supplemented HCD, or a tristearin-supplemented HCD and measured plasma FGF21 levels. Moreover, we examined the effect of SCD1 substrate (C18:0) on plasma FGF21 levels. Feeding the triolein-supplemented HCD was sufficient to reduce plasma FGF21 levels in LKO mice to those observed in LOX animals (Fig. 5*A*). Furthermore, triolein restored blood glucose levels in LKO mice to control levels, suggesting that hepatic SCD1 deficiency may modulate glucose uptake through FGF21 (Fig. 5*B*). In contrast, the tristearin-supplemented HCD failed to reduce plasma FGF21 levels to control levels (Fig. 5*B*). Because SCD1 synthesizes oleate and palmitoleate, we sought to examine the differential effects of these fatty acids on hepatic FGF21 expression. For this, we reverted to cell culture studies. Primary hepatocytes treated with an SCD1 inhibitor were evaluated for FGF21 expression with or without supplementation with SCD1 substrates or products. Our study demonstrated that SCD1 inhibition resulted in induction of FGF21 expression. Remarkably, this induction was suppressed by oleate but not palmitoleate or palmitate treatment. Treatment with palmitate resulted in higher FGF21 expression in SCD-deficient hepatocytes (Fig. 5*C*). These data indicate that reduced oleate levels in response to SCD1 deficiency increase FGF21 expression and decrease blood glucose levels.

Oleate regulates FGF21 partially through PGC-1α

Hepatic SCD1 deficiency increases PGC-1α expression (Fig. 6*A*), consistent with previous reports (14). Restoring oleate levels either through endogenous or exogenous resources reduced PGC-1α in the liver of SCD1 KO mice. Because increased PGC-1α in the liver has been reported previously to increase FGF21 expression (20), we examined the expression of FGF21 in the liver and plasma of mice deficient in both SCD1 and PGC-1α (DLKO) mice fed the HCD for 14 days. Our results revealed that PGC-1α deletion decreased FGF21 expression in the liver and plasma of SCD1 KO mice (Fig. 4*B*) and reduced GLUT4 expression in WAT (Fig. 6*C*). DLKO mice also showed partial restoration (~25%) of basal glucose levels (Fig. 6*D*). The data indicate that hepatic SCD1 deficiency decreases oleate synthesis and increases FGF21 expression in the liver, at least in part through PGC-1α. These changes are expected to increase glucose uptake in adipose tissue either directly or indirectly (Fig. 6*E*).

Discussion

SCD1 deletion protects against diet-induced adiposity, increases insulin sensitivity, and improves glucose metabolism, implicating SCD1 in the development of metabolic diseases (11, 12). SCD1 GKO mice demonstrate enhanced glucose uptake in the heart and peripheral tissue, including BAT and skeletal muscle (12, 17). Increased glucose uptake in skeletal muscle and BAT correlated with increased insulin signaling and increased glycogen accumulation (12, 17). The mechanism by which SCD1 deficiency mediates these phenotypes is unclear. Also, the individual contribution of SCD1 from different tissues to these phenotypes has not yet been determined. Here we show that hepatic SCD1 deficiency enhances glucose uptake in the liver and adipose tissue through two distinct mechanisms. The first involves up-regulation of GLUT1 expression in the liver, whereas, in the second, GLUT4 expression is elevated in adipose tissue. Our findings indicate that enhanced systemic glucose uptake in the hepatic SCD1-deficient model is associated with elevated plasma FGF21 and adiponectin levels.

The data presented here support a role of fatty acids in the regulation of glucose metabolism, at least in part through modulation of genes encoding glucose transporters. We showed previously that reduced MUFA levels increase GLUT1 expression in adipose tissue of adipose-specific SCD1 knockout mice and *in vitro* in SCD1 inhibitor–treated differentiated 3T3L1 cells (21). This indicates that reduced MUFA levels induce tissue-specific, or localized, glucose uptake by increasing GLUT1 expression. Consistent with these results, GLUT1 inhibition results in significant suppression of glucose uptake in the livers of LKO mice. Even though SCD1 deficiency increased glucose uptake in the liver, our previous work showed no change in hepatic glucokinase gene expression (15). This may suggest that it is the enhanced GK activity that leads to higher glu-

Figure 2. Hepatic SCD1 deficiency differentially regulates genes encoding glucose transporters in metabolic tissues. 12-week-old LOX and LKO male mice were fed an HCD for 10–14 days, and mice were fasted 4 h before collecting tissues for analysis. *A* and *B*, liver and WAT gene expression analysis for the indicated genes using qPCR. Values are mean ± S.E. (n = 6–9/group) expressed as arbitrary units (*AU*). *C* and *D*, Western blotting with the indicated antibodies performed on white and brown adipose tissues. Values are mean ± S.E. (n = 3–5/group). *E* and *F*, white and brown adipose tissue gene expression analysis for the indicated lipogenic genes using qPCR. Values are mean ± S.E. (n = 7–9/group). *, $p < 0.05$; ***, $p < 0.001$ *versus* LOX counterparts by Student's two-tailed t test.

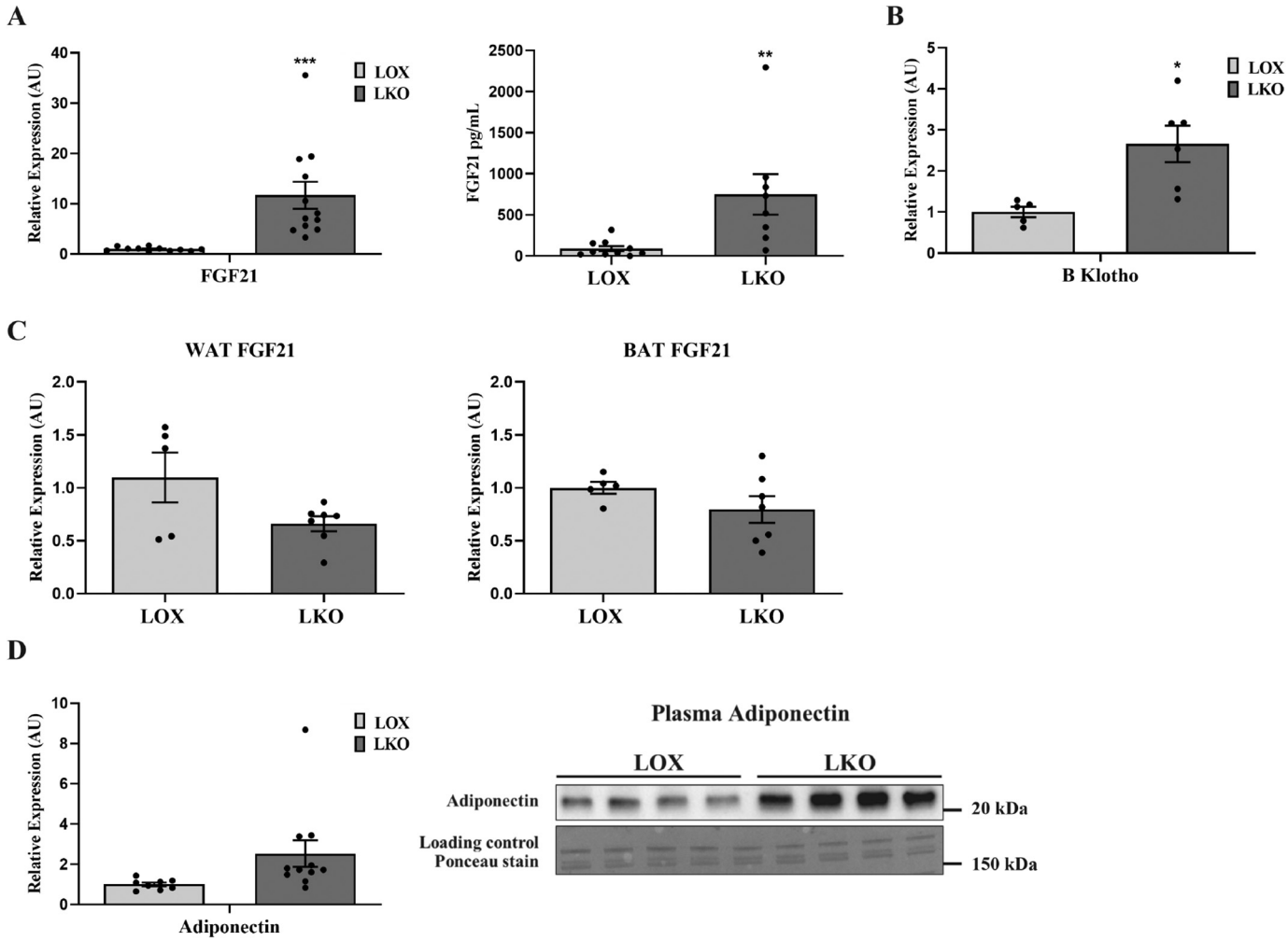

Figure 4. Hepatic SCD1 deficiency induces FGF21 expression. 10-week-old LOX and LKO male mice were fed an HCD for 10 days, and mice were fasted 4 h before collecting tissues for analysis. *A*, relative FGF21 expression in liver and plasma. *B*, hepatic gene expression of KLB. *C*, relative FGF21 expression in white and brown adipose tissue. *D*, relative adiponectin expression in white adipose tissue and adiponectin plasma levels ($n = 7–8$/group). Values are mean ± S.E. *, $p < 0.05$; **, $p < 0.01$; ***, $p < 0.001$ *versus* LOX counterparts by Student's two-tailed *t* test. *AU*, arbitrary units.

cose metabolism and, subsequently, the hypoglycemia observed in LKO mice. However, this inference requires further investigation.

We previously reported that SCD1 GKO mice showed enhanced GLUT4 expression in adipose tissue (17, 21). The induction of GLUT4 expression in adipose tissue of LKO mice indicates that reducing hepatic MUFA synthesis is sufficient to recapitulate the increased glucose uptake phenotype observed in adipose tissue of SCD1 GKO mice. Analysis of plasma fatty acid composition revealed that hepatic SCD1 deficiency was associated with reduced oleate levels (14). Increased GLUT4 expression may allow a shift in adipose tissue fuel metabolism to compensate for reduced plasma oleate levels. Accordingly, oleate treatment decreases GLUT4 expression in differentiated 3T3L1 cells (22). Thus, reduced hepatic oleate synthesis and transport may increase glucose uptake and metabolism in WAT of LKO mice. These data build on the previously described notion of a reciprocal relationship between glucose and fatty acid metabolism in adipose tissue (23). In addition, LKO mice fed an HCD demonstrate improved glucose tolerance, suggesting that enhanced insulin sensitivity might contribute to increased glucose metabolism in adipose tissue (14). Active insulin signaling stimulates GLUT4 translocation to the plasma membrane and subsequently increases glucose uptake in adipose tissue (24–27).

Our data provide evidence of the involvement of fatty acid in the regulation of FGF21 expression. SCD1 deficiency causes a significant reduction in the MUFA-to-SFA ratio, which suggests that increased FGF21 is either a result of reduced MUFA levels or accumulated SFA. However, the failure of the tristearin-supplemented HCD to cause further elevation of FGF21 in LKO mice suggests that the SCD1-mediated increase in plasma FGF21 is due to reduced MUFA levels but not accumulated SFA. Consistently, feeding a triolein-supplemented HCD normalized plasma FGF21 in LKO mice to control levels, suggesting that SCD1 deficiency–induced reduction of hepatic oleate levels increases FGF21 expression. This may partially explain why SCD1 GKO mice on a methionine-restricted diet showed reduced hepatic FGF21 expression (28). In support of this, oleate but not palmitoleate treatment suppressed SCD1 inhibitor–induced FGF21 expression in isolated primary hepatocytes. Cells cotreated with an SCD1 inhibitor and palmitate

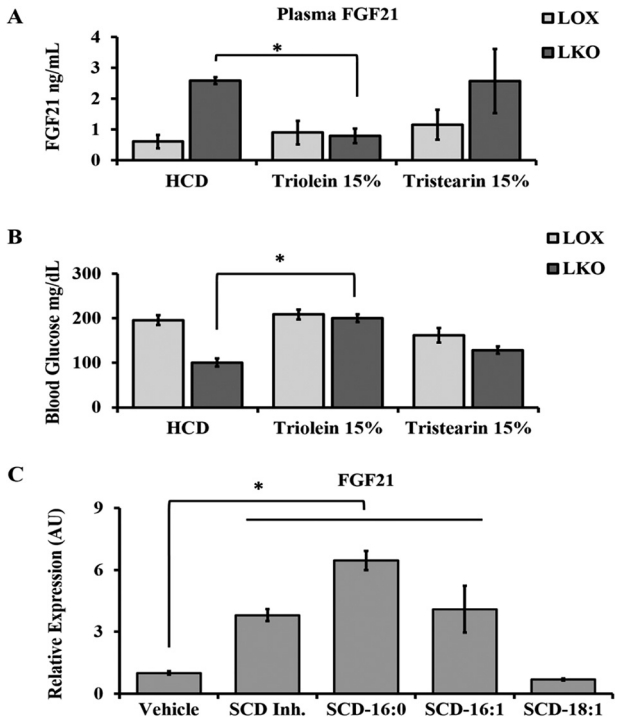

Figure 5. Oleate is a critical regulator of FGF21 expression. 12-week-old LOX and LKO mice were fed either an HCD, triolein, or tristearin for 10 days. Mice were euthanized after 4 h of fasting, and plasma samples were collected. *A* and *B*, relative FGF21 expression and plasma protein levels (*A*) and blood glucose levels (*B*) after 4 h of fasting. Values are mean ± S.E. ($n = 3$–5/group). *, $p < 0.05$ *versus* LOX counterparts by Student's two-tailed *t* test. *C*, FGF21 expression in primary hepatocytes treated with an SCD1 inhibitor (*SCD Inh*) or SCD1 inhibitor in combination with palmitate (*16:0*), palmitoleate (*16:1*), or oleate (*18:1*).

resulted in higher FGF21 expression compared with SCD1 inhibitor–treated cells. In the diet-induced obesity mouse model, palmitoleate treatment increased FGF21 expression compared with oleate (29). These results contradict previously reported *in vitro* work showing that treating HepG2 cells with oleate but not palmitate increased FGF21 expression (30). Even though more studies are required to further characterize the effect of oleate on FGF21 expression, feeding a triolein-supplemented diet did not cause a significant elevation in FGF21 relative to HCD-fed control mice.

PGC-1α regulates the expression of multiple genes involved in lipid and glucose metabolism. In patients with nonalcoholic fatty liver diseases, low PGC-1α expression is associated with insulin resistance (31). Increased FGF21 correlates with increased ER stress in the liver of LKO mice, and both of them are restored to normal levels upon restoring oleate levels (14). Hepatic oleate regulates ER stress through PGC-1α, which is also known to regulate liver FGF21 (14, 31). PGC-1α deletion was sufficient to relieve ER stress in the liver of LKO mice and reduce FGF21 expression. Taken together, these data reveal that PGC-1α–mediated ER stress (14, 32, 33) increases FGF21 expression in SCD1-deficient liver. Furthermore, reduced GLUT4 expression in adipose tissue in response to hepatic PGC-1α deletion may explain partial restoration of plasma glucose levels in DLKO mice. This result may further support FGF21 regulation of GLUT4 expression in WAT. Previously, we showed that hepatic SCD1 decreases protein expression of ChREBP and that feeding a triolein-supplemented diet restores its expression (15). Therefore, in LKO mice fed an HCD, the transcription factor ChREBP is less likely to be involved in SCD1 deficiency–induced FGF21 expression. In humans and mice, consumption of an HCD increases the expression of ChREBP and induces FGF21 (34).

FGF21 regulates systemic glucose metabolism (35, 36). Treatment with FGF21 results in decreased body weight, reduced blood glucose, and increased insulin sensitivity in the obese mouse model (37–40). Therefore, elevated plasma FGF21 in the SCD1-deficient state may contribute to the improved insulin sensitivity and enhanced glucose uptake observed in LKO mice. Taken together, our findings indicate that hepatic oleate is a critical regulator of glucose homeostasis.

Experimental procedures

Animal and diets

All experiments were carried out using the C57BL/6 mice background. The process of generating SCD1$^{lox/lox}$ (LOX) control mice and SCD1$^{lox/lox}$; Albumin Cre/+ tissue-specific liver knockout (SCD1 LKO) mice as well as SCD1 and PGC-1α double liver knockout mice (DLKO) has been described previously (14, 15). Mice were maintained at the University of Wisconsin-Madison animal care facility on regular 12 h light/dark cycles with free access to food and water. Mice were fed a standard rodent chow diet (Purina 5008) unless otherwise stated. All studies were carried out using 8- to 14-week-old mice. For experiments, mice were fed an HCD, which has very low fat, for a period of 10 days and fasted 4 h before being euthanized with an isoflurane overdose. Triolein- and tristearin-supplemented HCDs were prepared by supplementing the fat-free basal mix (TD88232, Harlan Teklad) with 15% by weight of tristearin (T5016, Sigma) or triolein (99% purity, T7140, Sigma). Collected tissues were snap-frozen in liquid nitrogen and stored at −80 °C for future analysis. All *in vivo* experimental animal procedures performed were approved by the Institutional Animal Care and Use Committee at the University of Wisconsin-Madison.

Fatty acid preparation and cell culture

Primary hepatocytes were derived from C57BL/6J mice. Briefly, mouse liver was initially perfused with perfusion buffer (400 ml of Hank's Balanced Salt Solution, 25 ml of HEPES (7.2 g/30 ml), and 5 ml of EGTA (95 mg/5 ml) (pH 7.5)). The liver was then perfused with collagenase buffer (80 ml of HBSS, 10 ml of $CaCl_2$ (74 mg/10 ml), and 5 ml of HEPES (pH 7.5)). Later, isolated hepatocytes were passed through a 70-μM cell strainer (Biosciences, South San Francisco, CA) and maintained in serum-free medium 199 (Invitrogen/Gibco, Grand Island, NY) for subsequent experiments (41).

Fatty acid stock solutions (1 mM) of palmitoleate and oleate were complexed to fatty acid–free BSA in 150 mM NaCl. The fatty acids and BSA stock mixtures were incubated at 37 °C for 1 h with constant vortexing. For the preparation of sodium palmitate BSA solution, sodium palmitate was dissolved in 150 mM NaCl solution at 70 °C for 30 min and then added to filtered fatty acid–free BSA solution while stirring at 37 °C for 1 h. This created a 1 mM sodium palmitate/0.17 mM BSA solution with a

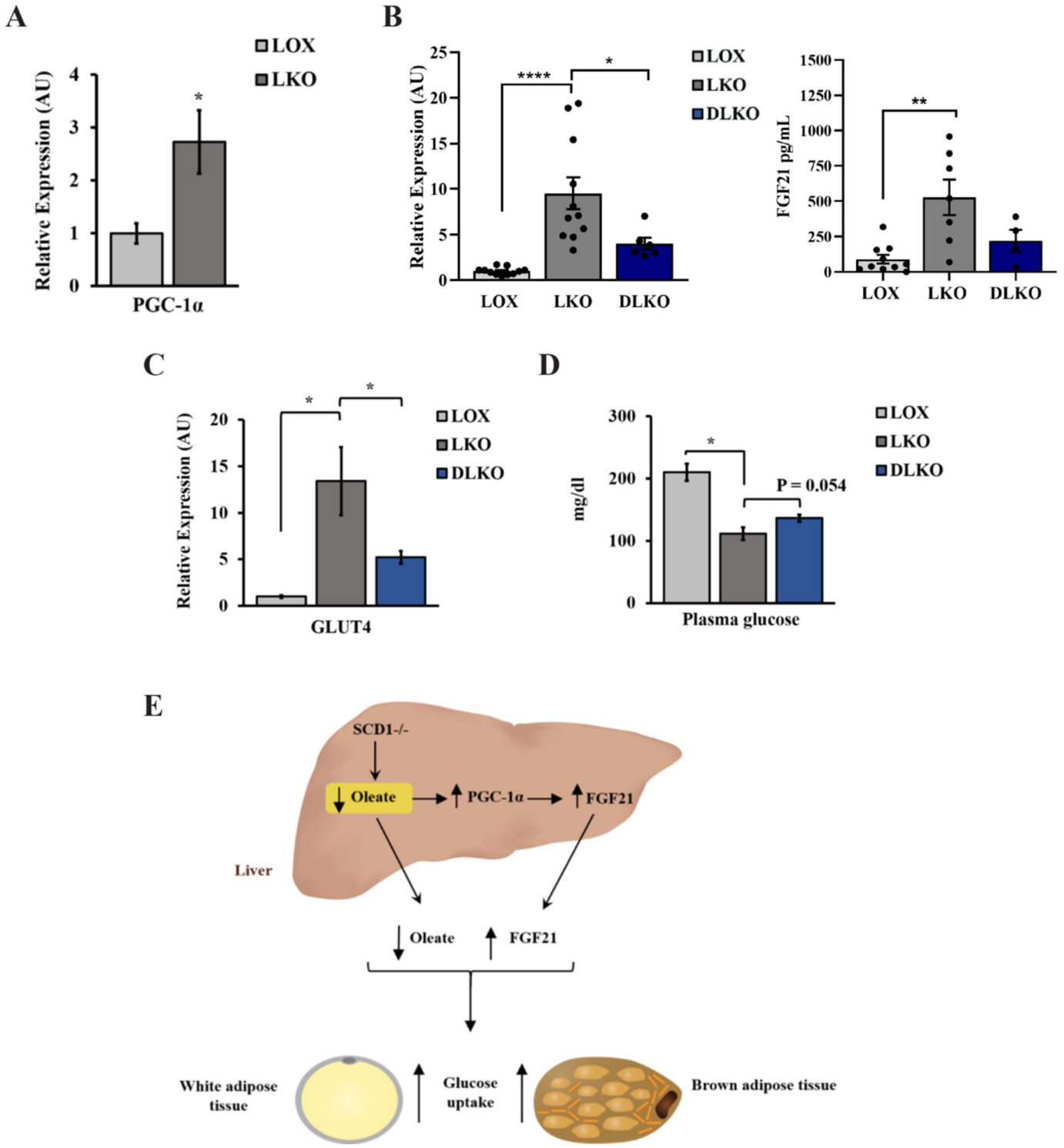

Figure 6. Oleate regulates FGF21 partially through PGC-1α. *A*, relative PGC-1α expression in the liver of 10-week-old LOX and LKO male mice fed an HCD for 14 days. *B*, relative hepatic and plasma FGF21 expression of LKO and DLKO mice. *C*, relative GLUT4 expression in WAT of LKO and DLKO mice expressed as arbitrary units (AU). *D*, plasma glucose levels in 12-week-old LOX, LKO, and DLKO male mice fed an HCD. Values are mean ± S.E. ($n = 8–10$/group). *, $p < 0.05$; **, $p < 0.01$; ****, $p < 0.0001$ *versus* LOX counterparts by Student's two-tailed *t* test. *E*, summary. Hepatic SCD1 deficiency decreases oleate synthesis and increases FGF21 expression in the liver through PGC-1α. These changes are expected to increase glucose uptake in liver and adipose tissue either directly or indirectly.

6:1 molar ratio of palmitate and BSA. Isolated primary hepatocytes were incubated overnight in serum-free DMEM and then treated with either 1 μM A939572 (an SCD1 inhibitor) alone or in combination with 100 μM BSA-conjugated fatty acids for 12 h before harvest.

Real-time quantitative PCR analysis

Total RNA isolation was performed using Tri reagent (Molecular Research Center) and subsequently treated with Turbo DNase (Ambion). Isolated RNA was reverse-transcribed with a high-capacity cDNA reverse transcription kit (Applied

Biosystems). Real-time quantitative PCR analysis was performed using SYBR Green Master Mix (Applied Biosystems) and an ABI 7500 instrument (Applied Biosystems). Relative expression levels were determined using the comparative threshold cycle value normalized to the housekeeping gene 18S. Primer sequences are available upon request.

Plasma FGF21 assay

Mouse blood samples were collected via cardiac puncture into EDTA-containing tubes. Collected plasma samples were snap-frozen in liquid nitrogen and stored at −80 °C for future analysis. Plasma FGF21 levels were measured using the FGF-21 Quantikine ELISA Kit (R&D Systems, MF2100).

Immunoblot analysis

An aliquot of frozen animal tissue was homogenized using a bead homogenizer (Omni International, Inc., Kennesaw, GA) in ice-cold Radioimmunoprecipitation buffer (Cell Signaling Technology, Inc. Danvers, MA) with 1 mM PMSF and protease inhibitor (Protease Inhibitor Mixture Set III, Calbiochem, La Jolla, CA). After homogenization, samples were centrifuged at 14,000 rpm for 20 min at 4 °C. For adipose tissues, samples were spun twice to ensure complete removal of residual lipids, and supernatant was collected each time. The supernatant was immediately stored at −80 °C. For immunoblot analysis, 20 or 30 μg of protein was resolved on 12% polyacrylamide gels and transferred to a nitrocellulose membrane. For plasma samples, 10 μg of protein was loaded on the gel. Membranes were incubated with primary antibody at 4 °C overnight, followed by incubation with anti-rabbit or anti-mouse secondary antibody–horseradish peroxidase conjugate. Anti-Glut4 (2213, 1/1000) was purchased from Cell Signaling Technology, Inc., and anti-vinculin (18058, 1/2000) was purchased from Abcam (Cambridge, UK). Blots were detected by chemiluminescence and autoradiography using Bio-Rad Gel Doc. For densitometry, values of target proteins were first divided by values for vinculin (loading control) and presented relative to their expression in control mice.

In vivo 2-[^{3}H]deoxyglucose uptake assay

An *in vivo* 2-[^{3}H]deoxyglucose uptake assay was performed as reported previously with minor changes (12). Briefly, mice were fed the HCD for 10 days and fasted 4 h before the experiment. An oral gavage dose of 15 μCi of 2-[^{3}H]deoxyglucose per mouse in 20% dextrose solution was administered, and mice were euthanized after 1.5 h with an isoflurane overdose. Isolated samples were digested with 1 M KOH and subsequently neutralized with 1 M HCl. Neutralized samples were mixed with scintillation reagent, and radioactivity was quantified in a liquid scintillation counter.

PET/CT imaging and analysis

After overnight fasting, mice received tail vein injections of either vehicle or phloretin (10 mg/kg of body weight). After 1 h, all mice received another tail vein injection of ~9 MBq of FDG 1 h before imaging (42, 43). Mice were anesthetized with 2% isoflurane gas mixed with oxygen until the time of imaging (42, 43). All images were obtained using Siemens Inveon Hybrid Micro PET/CT (Siemens Medical Solutions, Knoxville, TN) in the prone position. Forty million counts per mouse were collected for the PET scan to obtain adequate signal to noise. PET data were histogrammed into a single frame and later restructured using ordered subset expectation maximization of three dimensions, followed by a maximum *posteriori* algorithm (matrix size, 128, 128, 159; pixel size, 0.776, 0.776, 0.796 mm; iterations. 18; subsets, 16; β smoothing factor, 0.004) with CT attenuation correction applied but no scatter correction (43, 44). Images were analyzed using the General Analysis tools provided by Siemens Inveon Research Workplace (Siemens Medical Solutions). Data were windowed identically and scaled based on each animal's decay-corrected injection activity. To avoid inaccuracies in quantitative measurements because of partial volume effects, three relatively small regions of interest (~⅓ the size of the tissue of interest) were drawn within the brain, kidneys, liver, heart, intestine, and WAT and then averaged. Regions of interest were quantified as the percent injected dose (ID) normalized by the mass of the tissue (percent ID per gram of tissue), assuming a tissue density of water of 1 g/ml.

Statistical analyses

Results are presented as mean ± S.E. Comparisons were performed using an unpaired, two-tailed Student's *t* test. Results with $p < 0.05$ were considered statistically significant compared with control LOX mice.

Author contributions—A. A. and J. M. N. conceptualization; A. A., M. I. K., A. B., C. G., L. O., D. N. S., S. A. L., and H. M. data curation; A. A., C. G., S. A. L., M. B., and H. M. formal analysis; A. A. and J. M. N. investigation; A. A., M. I. K., A. B., C. G., J. J., L. O., D. N. S., M. B., and H. M. methodology; A. A. and J. M. N. writing-original draft; D. N. S., H. M., and J. M. N. resources; S. A. L., H. M., and J. M. N. writing-review and editing; J. M. N. supervision; J. M. N. funding acquisition; J. M. N. project administration.

Acknowledgment—We thank Laura Vanderploeg (University of Wisconsin-Madison Biochemistry Department Media Center) for help with the design and production of figures.

References

1. Bagby, S. P. (2004) Obesity-initiated metabolic syndrome and the kidney: a recipe for chronic kidney disease? *J. Am. Soc. Nephrol.* **15,** 2775–2791 CrossRef Medline
2. Perry, R. J., Samuel, V. T., Petersen, K. F., and Shulman, G. I. (2014) The role of hepatic lipids in hepatic insulin resistance and type 2 diabetes. *Nature* **510,** 84–91 CrossRef Medline
3. Donnelly, K. L., Smith, C. I., Schwarzenberg, S. J., Jessurun, J., Boldt, M. D., and Parks, E. J. (2005) Sources of fatty acids stored in liver and secreted via lipoproteins in patients with nonalcoholic fatty liver disease. *J. Clin. Invest.* **115,** 1343–1351 CrossRef Medline
4. Higuchi, N., Kato, M., Shundo, Y., Tajiri, H., Tanaka, M., Yamashita, N., Kohjima, M., Kotoh, K., Nakamuta, M., Takayanagi, R., and Enjoji, M. (2008) Liver X receptor in cooperation with SREBP-1c is a major lipid synthesis regulator in nonalcoholic fatty liver disease. *Hepatol. Res.* **38,** 1122–1129 CrossRef Medline
5. Yew Tan, C., Virtue, S., Murfitt, S., Roberts, L. D., Robert, L. D., Phua, Y. H., Dale, M., Griffin, J. L., Tinahones, F., Scherer, P. E., and Vidal-Puig, A. (2015) Adipose tissue fatty acid chain length and mono-unsaturation increases with obesity and insulin resistance. *Sci. Rep.* **5,** 18366 CrossRef Medline

6. Warensjö, E., Risérus, U., and Vessby, B. (2005) Fatty acid composition of serum lipids predicts the development of the metabolic syndrome in men. *Diabetologia* **48,** 1999–2005 CrossRef Medline
7. Sjögren, P., Sierra-Johnson, J., Gertow, K., Rosell, M., Vessby, B., de Faire, U., Hamsten, A., Hellenius, M. L., and Fisher, R. M. (2008) Fatty acid desaturases in human adipose tissue: relationships between gene expression, desaturation indexes and insulin resistance. *Diabetologia* **51,** 328–335 CrossRef Medline
8. Mar-Heyming, R., Miyazaki, M., Weissglas-Volkov, D., Kolaitis, N. A., Sadaat, N., Plaisier, C., Pajukanta, P., Cantor, R. M., de Bruin, T. W., Ntambi, J. M., and Lusis, A. J. (2008) Association of stearoyl-CoA desaturase 1 activity with familial combined hyperlipidemia. *Arterioscler. Thromb. Vasc. Biol.* **28,** 1193–1199 CrossRef Medline
9. Jeyakumar, S. M., Lopamudra, P., Padmini, S., Balakrishna, N., Giridharan, N. V., and Vajreswari, A. (2009) Fatty acid desaturation index correlates with body mass and adiposity indices of obesity in Wistar NIN obese mutant rat strains WNIN/Ob and WNIN/GR-Ob. *Nutr. Metab. (Lond.)* **6,** 27 CrossRef Medline
10. Attie, A. D., Krauss, R. M., Gray-Keller, M. P., Brownlie, A., Miyazaki, M., Kastelein, J. J., Lusis, A. J., Stalenhoef, A. F., Stoehr, J. P., Hayden, M. R., and Ntambi, J. M. (2002) Relationship between stearoyl-CoA desaturase activity and plasma triglycerides in human and mouse hypertriglyceridemia. *J. Lipid Res.* **43,** 1899–1907 CrossRef Medline
11. Ntambi, J. M., Miyazaki, M., Stoehr, J. P., Lan, H., Kendziorski, C. M., Yandell, B. S., Song, Y., Cohen, P., Friedman, J. M., and Attie, A. D. (2002) Loss of stearoyl-CoA desaturase-1 function protects mice against adiposity. *Proc. Natl. Acad. Sci. U.S.A.* **99,** 11482–11486 CrossRef Medline
12. Rahman, S. M., Dobrzyn, A., Dobrzyn, P., Lee, S. H., Miyazaki, M., and Ntambi, J. M. (2003) Stearoyl-CoA desaturase 1 deficiency elevates insulin-signaling components and down-regulates protein-tyrosine phosphatase 1B in muscle. *Proc. Natl. Acad. Sci. U.S.A.* **100,** 11110–11115 CrossRef Medline
13. Dobrzyn, P., Sampath, H., Dobrzyn, A., Miyazaki, M., and Ntambi, J. M. (2008) Loss of stearoyl-CoA desaturase 1 inhibits fatty acid oxidation and increases glucose utilization in the heart. *Am. J. Physiol. Endocrinol. Metab.* **294,** E357–E364 CrossRef Medline
14. Liu, X., Burhans, M. S., Flowers, M. T., and Ntambi, J. M. (2016) Hepatic oleate regulates liver stress response partially through PGC-1α during high-carbohydrate feeding. *J. Hepatol.* **65,** 103–112 CrossRef Medline
15. Miyazaki, M., Flowers, M. T., Sampath, H., Chu, K., Otzelberger, C., Liu, X., and Ntambi, J. M. (2007) Hepatic stearoyl-CoA desaturase-1 deficiency protects mice from carbohydrate-induced adiposity and hepatic steatosis. *Cell Metab.* **6,** 484–496 CrossRef Medline
16. Lee, S. H., Dobrzyn, A., Dobrzyn, P., Rahman, S. M., Miyazaki, M., and Ntambi, J. M. (2004) Lack of stearoyl-CoA desaturase 1 upregulates basal thermogenesis but causes hypothermia in a cold environment. *J. Lipid Res.* **45,** 1674–1682 CrossRef Medline
17. Rahman, S. M., Dobrzyn, A., Lee, S. H., Dobrzyn, P., Miyazaki, M., and Ntambi, J. M. (2005) Stearoyl-CoA desaturase 1 deficiency increases insulin signaling and glycogen accumulation in brown adipose tissue. *Am. J. Physiol. Endocrinol. Metab.* **288,** E381–E387 CrossRef Medline
18. Saeidi, N., Meoli, L., Nestoridi, E., Gupta, N. K., Kvas, S., Kucharczyk, J., Bonab, A. A., Fischman, A. J., Yarmush, M. L., and Stylopoulos, N. (2013) Reprogramming of intestinal glucose metabolism and glycemic control in rats after gastric bypass. *Science* **341,** 406–410 CrossRef Medline
19. Lin, Z., Tian, H., Lam, K. S., Lin, S., Hoo, R. C., Konishi, M., Itoh, N., Wang, Y., Bornstein, S. R., Xu, A., and Li, X. (2013) Adiponectin mediates the metabolic effects of FGF21 on glucose homeostasis and insulin sensitivity in mice. *Cell Metab.* **17,** 779–789 CrossRef Medline
20. Cornu, M., Oppliger, W., Albert, V., Robitaille, A. M., Trapani, F., Quagliata, L., Fuhrer, T., Sauer, U., Terracciano, L., and Hall, M. N. (2014) Hepatic mTORC1 controls locomotor activity, body temperature, and lipid metabolism through FGF21. *Proc. Natl. Acad. Sci. U.S.A.* **111,** 11592–11599 CrossRef Medline
21. Hyun, C. K., Kim, E. D., Flowers, M. T., Liu, X., Kim, E., Strable, M., and Ntambi, J. M. (2010) Adipose-specific deletion of stearoyl-CoA desaturase 1 up-regulates the glucose transporter GLUT1 in adipose tissue. *Biochem. Biophys. Res. Commun.* **399,** 480–486 CrossRef Medline
22. Long, S. D., and Pekala, P. H. (1996) Regulation of GLUT4 gene expression by arachidonic acid: evidence for multiple pathways, one of which requires oxidation to prostaglandin E2. *J. Biol. Chem.* **271,** 1138–1144 CrossRef Medline
23. Randle, P. J., Garland, P. B., Hales, C. N., and Newsholme, E. A. (1963) The glucose fatty-acid cycle: its role in insulin sensitivity and the metabolic disturbances of diabetes mellitus. *Lancet* **1,** 785–789 Medline
24. Sano, H., Eguez, L., Teruel, M. N., Fukuda, M., Chuang, T. D., Chavez, J. A., Lienhard, G. E., and McGraw, T. E. (2007) Rab10, a target of the AS160 Rab GAP, is required for insulin-stimulated translocation of GLUT4 to the adipocyte plasma membrane. *Cell Metab.* **5,** 293–303 CrossRef Medline
25. Hill, M. M., Clark, S. F., Tucker, D. F., Birnbaum, M. J., James, D. E., and Macaulay, S. L. (1999) A role for protein kinase Bβ/Akt2 in insulin-stimulated GLUT4 translocation in adipocytes. *Mol. Cell. Biol.* **19,** 7771–7781 CrossRef Medline
26. Kohn, A. D., Summers, S. A., Birnbaum, M. J., and Roth, R. A. (1996) Expression of a constitutively active Akt Ser/Thr kinase in 3T3-L1 adipocytes stimulates glucose uptake and glucose transporter 4 translocation. *J. Biol. Chem.* **271,** 31372–31378 CrossRef Medline
27. Quon, M. J., Butte, A. J., Zarnowski, M. J., Sesti, G., Cushman, S. W., and Taylor, S. I. (1994) Insulin receptor substrate 1 mediates the stimulatory effect of insulin on GLUT4 translocation in transfected rat adipose cells. *J. Biol. Chem.* **269,** 27920–27924 Medline
28. Forney, L. A., Stone, K. P., Wanders, D., Ntambi, J. M., and Gettys, T. W. (2018) The role of suppression of hepatic SCD1 expression in the metabolic effects of dietary methionine restriction. *Appl. Physiol. Nutr. Metab.* **43,** 123–130 CrossRef Medline
29. de Souza, C. O., Teixeira, A. A. S., Biondo, L. A., Lima Junior, E. A., Batatinha, H. A. P., and Rosa Neto, J. C. (2017) Palmitoleic acid improves metabolic functions in fatty liver by PPARα-dependent AMPK activation. *J. Cell. Physiol.* **232,** 2168–2177 CrossRef Medline
30. Mai, K., Andres, J., Biedasek, K., Weicht, J., Bobbert, T., Sabath, M., Meinus, S., Reinecke, F., Möhlig, M., Weickert, M. O., Clemenz, M., Pfeiffer, A. F., Kintscher, U., Spuler, S., and Spranger, J. (2009) Free fatty acids link metabolism and regulation of the insulin-sensitizing fibroblast growth factor-21. *Diabetes* **58,** 1532–1538 CrossRef Medline
31. Koliaki, C., Szendroedi, J., Kaul, K., Jelenik, T., Nowotny, P., Jankowiak, F., Herder, C., Carstensen, M., Krausch, M., Knoefel, W. T., Schlensak, M., and Roden, M. (2015) Adaptation of hepatic mitochondrial function in humans with non-alcoholic fatty liver is lost in steatohepatitis. *Cell Metab.* **21,** 739–746 CrossRef Medline
32. Jiang, S., Yan, C., Fang, Q. C., Shao, M. L., Zhang, Y. L., Liu, Y., Deng, Y. P., Shan, B., Liu, J. Q., Li, H. T., Yang, L., Zhou, J., Dai, Z., Liu, Y., and Jia, W. P. (2014) Fibroblast growth factor 21 is regulated by the IRE1α-XBP1 branch of the unfolded protein response and counteracts endoplasmic reticulum stress-induced hepatic steatosis. *J. Biol. Chem.* **289,** 29751–29765 CrossRef Medline
33. Schaap, F. G., Kremer, A. E., Lamers, W. H., Jansen, P. L., and Gaemers, I. C. (2013) Fibroblast growth factor 21 is induced by endoplasmic reticulum stress. *Biochimie* **95,** 692–699 CrossRef Medline
34. Fisher, F. M., Kim, M., Doridot, L., Cunniff, J. C., Parker, T. S., Levine, D. M., Hellerstein, M. K., Hudgins, L. C., Maratos-Flier, E., and Herman, M. A. (2017) A critical role for ChREBP-mediated FGF21 secretion in hepatic fructose metabolism. *Mol. Metab.* **6,** 14–21 CrossRef Medline
35. Xu, J., Lloyd, D. J., Hale, C., Stanislaus, S., Chen, M., Sivits, G., Vonderfecht, S., Hecht, R., Li, Y. S., Lindberg, R. A., Chen, J. L., Jung, D. Y., Zhang, Z., Ko, H. J., Kim, J. K., and Véniant, M. M. (2009) Fibroblast growth factor 21 reverses hepatic steatosis, increases energy expenditure, and improves insulin sensitivity in diet-induced obese mice. *Diabetes* **58,** 250–259 CrossRef Medline
36. Liu, M., Cao, H., Hou, Y., Sun, G., Li, D., and Wang, W. (2018) Liver plays a major role in FGF-21 mediated glucose homeostasis. *Cell Physiol. Biochem.* **45,** 1423–1433 CrossRef Medline
37. Chau, M. D., Gao, J., Yang, Q., Wu, Z., and Gromada, J. (2010) Fibroblast growth factor 21 regulates energy metabolism by activating the AMPK-

SIRT1-PGC-1α pathway. *Proc. Natl. Acad. Sci. U.S.A.* **107,** 12553–12558 CrossRef Medline

38. Xu, J., Stanislaus, S., Chinookoswong, N., Lau, Y. Y., Hager, T., Patel, J., Ge, H., Weiszmann, J., Lu, S. C., Graham, M., Busby, J., Hecht, R., Li, Y. S., Li, Y., Lindberg, R., and Véniant, M. M. (2009) Acute glucose-lowering and insulin-sensitizing action of FGF21 in insulin-resistant mouse models: association with liver and adipose tissue effects. *Am. J. Physiol. Endocrinol. Metab.* **297,** E1105–E1114 CrossRef Medline
39. Vernia, S., Cavanagh-Kyros, J., Garcia-Haro, L., Sabio, G., Barrett, T., Jung, D. Y., Kim, J. K., Xu, J., Shulha, H. P., Garber, M., Gao, G., and Davis, R. J. (2014) The PPARα-FGF21 hormone axis contributes to metabolic regulation by the hepatic JNK signaling pathway. *Cell Metab.* **20,** 512–525 CrossRef Medline
40. Guridi, M., Tintignac, L. A., Lin, S., Kupr, B., Castets, P., and Rüegg, M. A. (2015) Activation of mTORC1 in skeletal muscle regulates whole-body metabolism through FGF21. *Sci. Signal.* **8,** ra113 CrossRef Medline
41. Lamming, D. W., Demirkan, G., Boylan, J. M., Mihaylova, M. M., Peng, T., Ferreira, J., Neretti, N., Salomon, A., Sabatini, D. M., and Gruppuso, P. A. (2014) Hepatic signaling by the mechanistic target of rapamycin complex 2 (mTORC2). *FASEB J.* **28,** 300–315 CrossRef Medline
42. Fueger, B. J., Czernin, J., Hildebrandt, I., Tran, C., Halpern, B. S., Stout, D., Phelps, M. E., and Weber, W. A. (2006) Impact of animal handling on the results of 18F-FDG PET studies in mice. *J. Nucl. Med.* **47,** 999–1006 Medline
43. García-Mendoza, M. G., Inman, D. R., Ponik, S. M., Jeffery, J. J., Sheerar, D. S., Van Doorn, R. R., and Keely, P. J. (2016) Neutrophils drive accelerated tumor progression in the collagen-dense mammary tumor microenvironment. *Breast Cancer Res.* **18,** 49 CrossRef Medline
44. Disselhorst, J. A., Brom, M., Laverman, P., Slump, C. H., Boerman, O. C., Oyen, W. J., Gotthardt, M., and Visser, E. P. (2010) Image-quality assessment for several positron emitters using the NEMA NU 4–2008 standards in the Siemens Inveon small-animal PET scanner. *J. Nucl. Med.* **51,** 610–617 CrossRef Medline